Size-dependent dynamic characteristics of graphene based multi-layer nano hetero-structures

Y. Chandra[a], T. Mukhopadhyay[b], S. Adhikari[a,*], L. Figiel[c]

[a] *Zienkiewicz Centre for Computational Engineering, Swansea University, Swansea SA1 8EN, UK*
[b] *Department of Aerospace Engineering, Indian Institute of Technology, Kanpur, India*
[c] *International Institute for Nanocomposite Manufacturing (IINM) & Warwick Center for Predictive Modelling, University of Warwick, CV4 7AL*

Abstract

Carbon-based nano hetero-structures are currently receiving increasing attention. In this paper, the vibration characteristics of graphene-hexagonal boron nitride (hBN) and graphene-molybdenum disulfide (MoS_2) are presented using atomistic finite element approach. Various possible scenarios, namely different geometrical configurations (armchair and zigzag), boundary conditions and aspect ratio are considered in the present study. The dynamic characteristics of nano hetero-structures studied have shown dependence on aspect ratio and the boundary conditions. Young's modulus (E) of the individual nanosheets significantly influences the vibrational behaviour of nano hetero-structures. Therefore, the values of E have also been predicted for individual sheets using atomistic simulations and correlated against the data in the literature. The natural frequencies of graphene-hBN nano hetero-structures predicted in the current work have been correlated against the molecular dynamics based studies available in the literature. The unique vibrational properties and large stiffness of nano hetero-structures identified in the present work make them a suitable candidate for manufacturing nanosensors, electromechanical resonators, and also will aid the nanomaterials research community to design various other nanodevices.

Keywords: 2D nanoparticles, hexagonal nano-structures, graphene, hexagonal boron nitride, molybdenum disulfide, nano hetero-structures, atomistic finite elements, dynamics of vibrations;

*Corresponding author. Tel: +44 (0)1792 602088, Fax: + 44 (0)1792 295676
Email address: S.Adhikari@swansea.ac.uk (S. Adhikari)

1. Introduction

Since the discovery of superlative monolayers and thin films of graphite [1, 2], research interest in the engineering and scientific applications of carbon nanostructures is growing. The superlatives identified in graphene has also lead to an increased interest in other possible two-dimensional materials that could offer exceptional electronic, optical, thermal, chemical and mechanical characteristics [3–5]. Since the last decade the curiosity in quasi-two-dimensional family of nano materials has grown from hexagonal boron nitride (hBN), boron-carbon-nitride (B-C-N), graphene oxides to chalcogenides such as molybdenum disulfide (MoS_2), molybdenum diselenide ($MoSe_2$), stanene, silicene, sermanene, phosphorene, borophene etc [6, 7]. It is essential to investigate these materials at nanoscale since the superlative properties appear in atomic scale and in single or few layer forms [8]. 2D nano materials researched in the literature are of various geometrical patterns and among these, hexagonally shaped nano-structures are of significance to the nano-technology research community [4]. Nano scale level continuum mechanics based models have evolved since the last decade, for graphene [9, 10] and hBN [11]. Although such single layer nano materials have been investigated using *ab initio* calculations [12–14], molecular dynamics (MD) [15–17] and molecular mechanics [18]. There is a limited literature available on the multi layer nano hetero-structures. The article by Zhang [19] is only research work that investigated vibrations behavior of van der Waals hetero-structures. This researcher used MD and continuum mechanics to determine natural frequencies of graphene-hBN and graphene-silicene hetero-structures. In the current article, the dynamic behavior of nano hetero-structures in terms of natural frequencies and mode shapes will be investigated using atomistic finite element method.

Table 1: Bond angles and sheet thickness for nano materials[20]. Refer Fig. 1 for angle representations.

Nanomaterial	α (in °)	θ (in °)	Sheet thickness (nm)
Graphene	0	120	0.34
hBN	0	120	0.098
MoS_2	48.15	120	0.603

This paper is organised as follows. In the second section, the derivation of mechanical properties of atomic bonds is shown. Followed by an overview on the atomistic simulation methodology utilized to model nano hetero-structures. This overview describes the finite element based atomistic modelling of individual sheets of graphene, hBN, MoS_2 and also the modeling of weak van der Waals interactions between them. The molecular representation of these distinct nano sheets

has been shown as isometric images in Fig. 3. The results and discussions have been presented in the fourth section. A comparison between the existing results in the literature and atomistically simulated E (Young's Modulus) has been given. The existing results in the literature are based on molecular dynamics/molecular mechanics (MD/MM), ab initio calculations and also analytical models. A comparison between natural frequencies obtained by MD simulations and atomistic FE simulations has also been given here. Wherein, the MD based solutions are obtained from the literature [19]. For this comparison study, a multilayered nano hetero-structure involving a layer of graphene and three layers of hBN is chosen. Then the first four mode shapes of graphene-hBN and graphene-MoS_2 are presented. This is followed by the results of detailed dynamic analysis of graphene-hBN and graphene-MoS_2 nano hetero-structures. These results investigate the influence of length, aspect ratio, boundary conditions and chirality on modal frequencies of nano hetero-stuctures. In the final section, concluding remarks have been given.

2. Mechanical equivalence of atomic bonds

In the case of atomic scale behaviour of materials, the total interatomic potential energy can be given as the sum of various individual energy terms relevant to bonding and non-bonding interactions [18]. Total strain energy (E_E) can be represented as the sum of energy contributions from bending of bonds (E_b), bond stretching (E_s), torsion of bonds (E_t) and energies associated with non-bonded terms (E_{nb}) such as the van der Waals attraction, the core repulsions and the Coulombic energy.

$$E_E = E_s + E_b + E_t + E_{nb} \tag{1}$$

The influence of bending and stretching is significant in case of small deformations as compared to all other energy components [10, 21]. For the case of multiplanar hexagonal nano-structures (such as MoS_2), the strain energy due to bending is comprised of two components, in-plane component (E_{bI}) and out-of-plane component (E_{bO}). The deformation mechanisms for the multiplanar nanostructure (MoS_2) are shown in Fig. 1 – 2. The out-of-plane angular component becomes zero for monoplanar nanostructures such as graphene and hBN. The total inter-atomic potential energy (E_E) can be represented as

$$\begin{aligned} E_E &= E_s + E_{bI} + E_{bO} \\ &= \frac{1}{2}k_r(\Delta l)^2 + \left(\frac{1}{2}k_\theta(\Delta\theta)^2 + \frac{1}{2}k_\theta(\Delta\alpha)^2\right) \end{aligned} \tag{2}$$

where Δl, $\Delta\theta$ and $\Delta\alpha$ denote the change in bond length, change in in-plane angle and change in out-of-plane angle respectively, as shown in Fig. 1. The quantities k_r and k_θ are the force

constants associated with bond stretching and bond bending respectively. The first term in Eq. 2 represents strain energy relevant to stretching (E_s), while the other terms represent the strain energies due to in-plane (E_{bI}) and out-of-plane (E_{bO}) angle variations, respectively. The force constants of the atomic bonds (k_r and k_θ) can be expressed in the form of structural equivalence [22]. As per the standard theory of classical structural mechanics (refer to Fig. 2), strain energy of a uniform circular beam with cross-sectional area A, length l, Young's modulus E, and second moment of area I, under the application of a pure axial force N (refer to Fig. 2(b)) can be expressed as

$$U_a = \frac{1}{2}\int_0^L \frac{N^2}{EA}\,\mathrm{d}l = \frac{1}{2}\frac{N^2 l}{EA} = \frac{1}{2}\frac{EA}{l}(\Delta l)^2 \tag{3}$$

The strain energies due to pure bending moment M (refer to Fig. 2(c)) can be written as

$$U_b = \frac{1}{2}\int_0^L \frac{M^2}{EI}\,\mathrm{d}l = \frac{1}{2}\frac{EI}{l}(2\Delta\phi)^2 \tag{4}$$

Comparing Eq. 3 with the expression for strain energy due to stretching (E_s) (refer Eq. 2), it

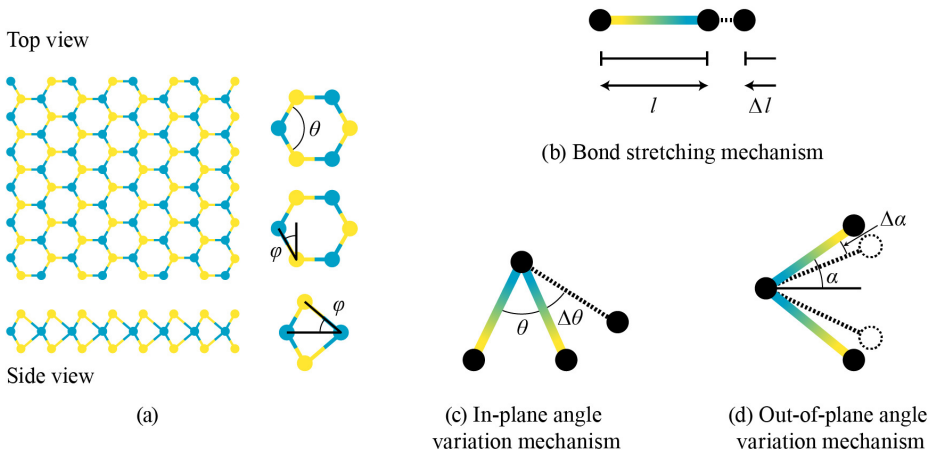

Fig. 1: (a) Different views of MoS_2 hexagonal nanostructure (b) Bond stretching induced strain energy (c) In-plane angle variation induced strain energy (d) Out-of-plane angle variation induced strain energy.

can be concluded that $K_r = \dfrac{EA}{l}$. For bending, it is reasonable to assume that $2\Delta\phi$ is equivalent to $\Delta\theta$ and $\Delta\alpha$ for in-plane and out-of-plane angle variations respectively (refer to Fig. 2(c)). Thus comparing Eq. 4 with the expressions for the strain energies due to in-plane (E_{bI}) and out-of-plane (E_{bO}) angle variations (refer Eq. 2), the following relation can be obtained: $k_\theta = \dfrac{EI}{l}$. There exists a mechanical equivalence between molecular mechanics parameters (k_r and k_θ) and structural mechanics parameters (EA and EI). Such mechanical equivalence can be used to derive beam (covalent bond) properties used in the atomistic simulations. In the current work, the effective elastic moduli and natural frequencies of nano hetero-structures are computed by

using these beams representing covalent bonds.

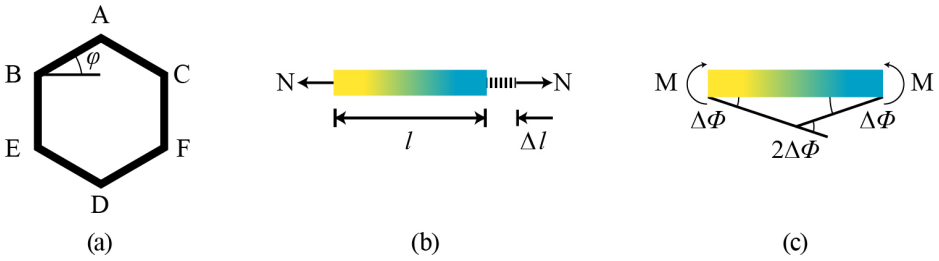

Fig. 2: (a) A hexagonal unit cell involving of 6 idealized beam elements (refer to Fig. 1(a)) (b) A beam element under the influence of pure tension (c) A beam element under the influence pure bending.

3. Atomistic FE models of nano hetero-structures using finite element method

The atomistic models deployed here are based on the finite element methodologies developed by the authors to study graphene and its associated nano structures [23–28]. In this research work, the finite element analysis tool OPTISTRUCT has been used to model the dynamic behaviour of nano hetero-structures. The covalent bonds are represented by 3D Timoshenko finite element beams and the atoms are represented by finite element nodes. Within the finite element analysis tool OPTISTRUCT, the element type CBEAM has been used to represent beams. The cross sectional diameter and the Young's modulus (E) of the beam elements are computed by using the equations of force-field constants K_r(stretching) and K_θ(torsional) shown in Section 2.

The numerical values of force constants K_r and K_θ are shown in the Table 2 and are taken from the literature [20]. By substituting these values in the equations $K_r = \frac{EA}{l}$ and $k_\theta = \frac{EI}{l}$, essential parameters to model covalent bonds such as beam diameter d and beam Young's modulus E can be calculated. The calculated values are shown in Table 2. Furthermore, the bond lengths, which are essentially beam lengths shown in Table 2 are also obtained from the literature [20]. From Table 2, it is evident that the nano material MoS_2 offers the highest interatomic bond length, while graphene offers the lowest bond lengths among the three materials considered in this work. The C-C bond length within graphene sheets is very close to that of B-N bond length in hBN sheets. Atomic masses of carbon, boron, nitrogen, molybdenum and sulphur have been considered by modeling mass elements on the nodes. The atomic masses prescribed are $1.9943X10^{-26}$ kg, $1.7952086X10^{-26}$ kg, $2.3258671X10^{-26}$ kg, $1.593121X10^{-25}$ kg and $1.593121X10^{-23}$ kg for carbon, boron, nitrogen, molybdenum and sulphur, respectively.

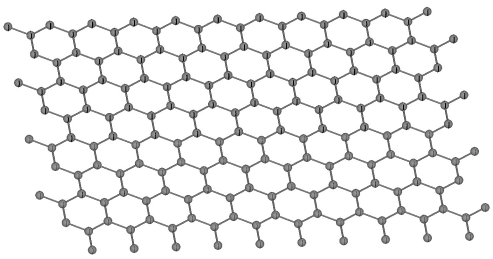

(a) Graphene

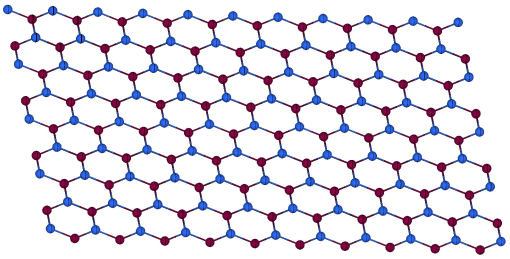

(b) Hexagonal Boron Nitride(Nitrogen in blue)

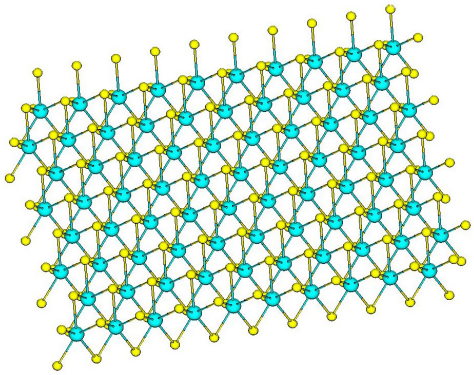

(c) Molybdenum disulphide(Molybdenum in green)

Fig. 3: Isometric views of graphene, hexagonal boron nitride sheets and molybdenum disulphide molecules.

Within the finite element analysis tool OPTISTRUCT, the element type CONM2 has been used to represent masses.

Table 2: Bond properties for each individual nano material[20].

Nanomaterial	K_r in N nm^{-1}	K_θ in N-nm-rad^{-2}	L in nm	d in nm	E in GPa
Graphene	$6.52e-7$	$8.76e-10$	0.142	0.146	1370.91
hBN	$4.86e-7$	$6.95e-10$	0.145	0.151	1047.1
MoS_2	$1.64e-7$	$1.67e-9$	0.242	0.403	882.1

The equivalent axial force for an L-J potential between pair of atoms (i, j) belonging to different nano sheets can be defined as [29]

$$F_{ij} = \frac{\partial V_{ij}}{\partial r} \tag{5}$$

where, r is the atomic displacement along ij (layer-layer length). As per Girifalco et al. [30], the force between the atoms (ij) can also be represented by

$$F_{ij} = -12\,\epsilon \left[\left(\frac{r_{min}}{y} \right)^{13} - \left(\frac{r_{min}}{y} \right)^{7} \right] \tag{6}$$

where, $y = r_{min} + \delta r$, δr is the atomic displacement along the length **ij**. The r_{min} (in Å) is given

by $2^{\frac{1}{6}}\,\sigma$, where $\sigma = (A/B)^{1/6}$. The B and A are attractive and repulsive constants, respectively. In the current research work, three different nano sheets have been considered namely graphene, hBN and MoS_2. Hetero-structures of graphene-hBN and graphene-MoS_2 have been studied under dynamic conditions. These hetero-structures lead to C-B, C-N, B-B, N-N, C-M, C-S, M-M, M-S and S-S atomic interactions. Where C,B,N,M and S are carbon, boron, nitrogen, molybdenum and sulphide atoms, respectively. The values of σ and ϵ for each individual van der Waals atomic interactions are given in Table 3. These values have been obtained from various references [31–34]. In the atomistic FE models, we have used spring elements to form a nonlinear connection between two layers of the bilayer structure representing L-J interactions. The force deflection curve for L-J springs has been calculated by using the relation in Eq. 6. These curves of L-J potential forces for each interlayer interaction obtained by Eq. 6 are shown in Fig. 4. Within the finite element analysis tool OPTISTRUCT, the L-J springs of interlayer interactions are modeled by element type CBUSH and by using the curves of Fig. 4 as input properties.

Table 3: Constants of LJ-potentials.

Nanomaterial	ϵ in meV	σ in $\mathring{A}$	Source
C-M	3.325	2.82	[31]
C-S	7.355	3.22	[31]
M-M	2.43	2.72	[32]
S-S	1.19	3.59	[32]
M-S	2.49	3.16	[32]
C-B	3.6	2.2132	[33]
C-N	9	3.2222	[33]
B-B	4.16	3.453	[34]
N-N	6.281	3.365	[34]

In the atomistic FE approach, coupled nano sheets of heterogenous nature are modeled as space-frame structures. Overall mass and stiffness matrices of the atomistic FE models are generated from the equivalent matrices of the beams representing C-C,C-S,M-M,S-S,M-S,C-B,C-N,B-B and N-N bonds and concentrated masses at each node. The lumped mass matrix for a single beam element can be represented as:

$$[\mathbf{M}]_{\mathbf{e}} = diag\left[\begin{array}{cccccc} \frac{m_a}{3} & \frac{m_a}{3} & \frac{m_a}{3} & 0 & 0 & 0 \end{array}\right] \tag{7}$$

Where m_a in kg is the mass of number of atoms. The general equation of motion of the undamped system ($[\mathbf{K}]\mathbf{x} + [\mathbf{M}]\ddot{\mathbf{x}} = \mathbf{0}$) leading to a standard undamped eigenvalue problem ($\left(\left[\mathbf{K}\right] - \omega^2\left[\mathbf{M}\right]\right)\{\mathbf{x}\} = \{\mathbf{0}\}$) has been solved using a block Lanczos algorithm within the finite element analysis code OPTISTRUCT.

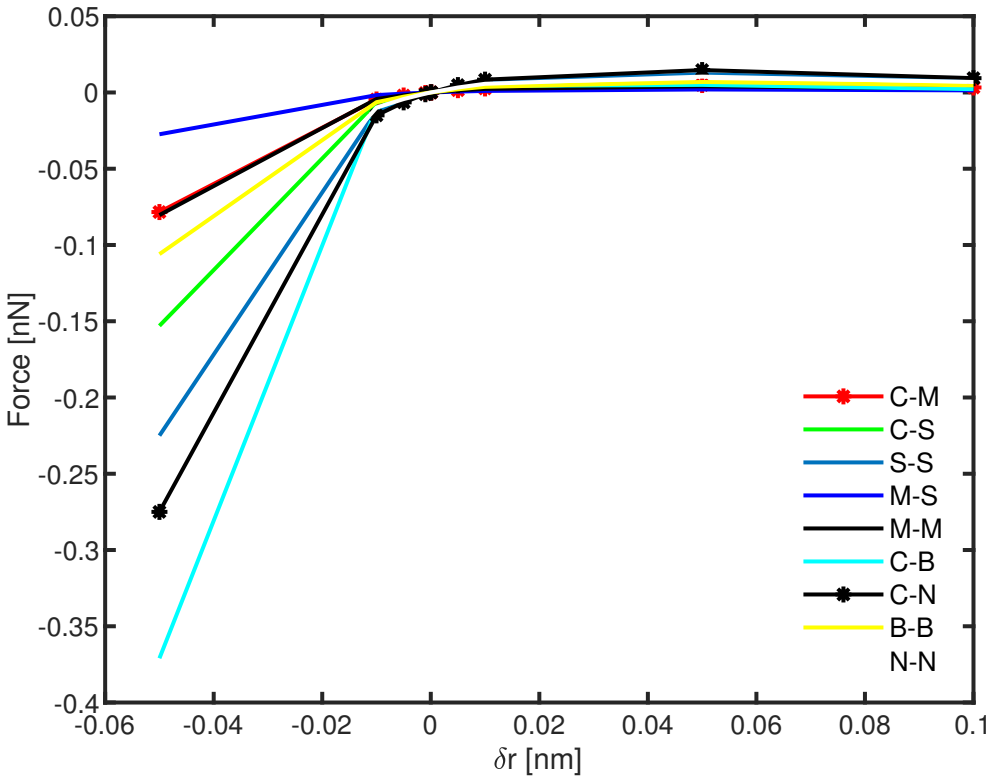

Fig. 4: Curves of L-J potential forces obtained by Eq. 6.

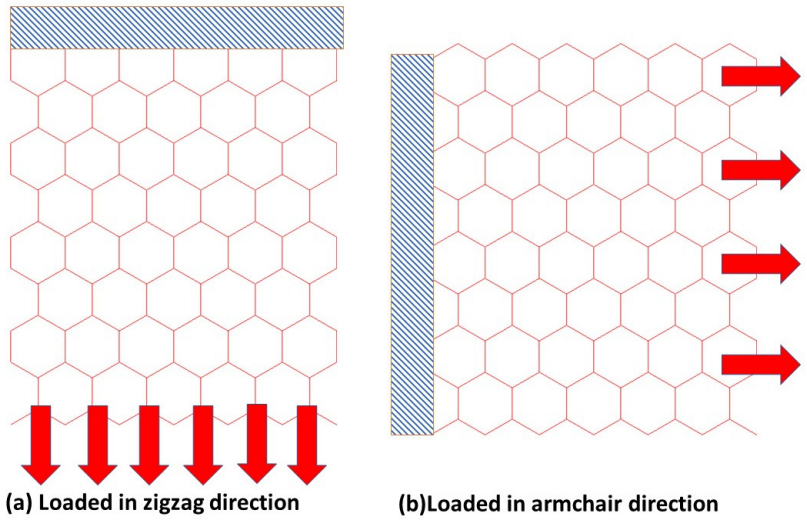

Fig. 5: Boundary conditions for elastic analysis (the marked edges are fully constrained in all six degrees of freedom.)

4. Results and discussions

4.1. Validation of Young's modulus of graphene, hBN and MoS_2

In this section, an analysis of elastic behaviour of graphene, hBN and MoS_2 has been presented. For each nano material, elastic analysis has been performed in zigzag and armchair directions. With respect to armchair and zigazag directions, one end of the nano sheet has been constrained and an unit load has been applied to other end. These boundary conditions have been depicted in Fig. 5. The resulting strain due to the applied unit load has been numerically calculated using the atomistic FEM. Based on this strain and applied stresses due to the unit load, the E has then been calculated. The E with respect to armchair direction has been referred to as E_1 and the E with respect to zigzag direction has been referred to as E_2. The tensile moduli E_1 and E_2 have been converted to tensile rigidities E_{1T} and E_{2T} by multiplying moduli terms with the sheet thickness shown in the Table 1. For the case of graphene and hBN sheets, 4 separate finite element models have been constructed with sheet sizes 1.775 nm $\times$ 3.074 nm, 1.775 nm $\times$ 3.813 nm, 1.775 nm $\times$ 4.55 nm and 1.775 nm $\times$ 5.534 nm. The largest among these four finite element models has resulted in upto 654 beam elements and 513 nodes. The aspect ratio of these four finite element models are 1.73, 2.14 , 2.56 and 3.11. Also, for the case of MoS_2 sheets, 4 seperate finite element models have been constructed with sheet sizes 1.483 nm $\times$ 2.625 nm, 1.483 nm $\times$ 2.94 nm, 1.483 nm $\times$ 3.359 nm and 1.483 nm $\times$ 4.199 nm. The largest among these four finite element models has resulted in upto 958 beam elements and 587 nodes. The aspect ratio of these four finite element models are 1.77, 1.98, 2.26 and 2.83. The variation of E_{1T} and E_{2T} against aspect ratio (AR) for all three nano materials are shown in Fig. 6. Within these plots, also presented are the E_{1T} and E_{2T} from the literature [20]. The authors [20] considered an analytical closed formula to determine unique values of E_{1T} and E_{2T} of graphene, hBN and MoS_2 by considering a single hexagonal unit cell of each nano material. Due to this fact, the curves from the literature [20] remain flat in the plots of Fig. 6. As per these plots, the numerically predicted values are very close to that of analytical prediction of literature. However, the numerically predicted values are found be lower as compared to analytical predictions of literature. The reason for such a behavior is twofold: first reason being the analytical predictions were based on single unit cell and second reason being the assumption of continuous behavior when the number of unit cells is increased to more than one. But within the atomistic simulations, multiple number of unit cells in each sheet are considered. Within the numerical models, higher the number of unit cells, higher will be the number of beam elements.

As the number of beam elements increases, more flexibility is added to the model. Such a flexibility (added degrees of freedom) can under-predict the elastic modulus of the nano structures. However, as per these plots, the increase in aspect ratio from 2.3 to 2.9 has led to a negligible increase in tensile rigidity. This indicates that, as the space frame lattice of nano strucutures becomes larger in dimension, it simulates a continuous plate. Similar behavior has also been observed for bilayer and single layer graphene sheets [24]. Furthermore, the numerically obtained single layer tensile rigidities have also been compared against the results from various other publications. This comparison is shown in Table 4. The publications present in the table cover *ab initio* calculations, molecular dynamic simulations and also experimental investigations. It can be concluded that the tensile rigidities calculated in the present work are closer to those calculated by non-numerical methods.

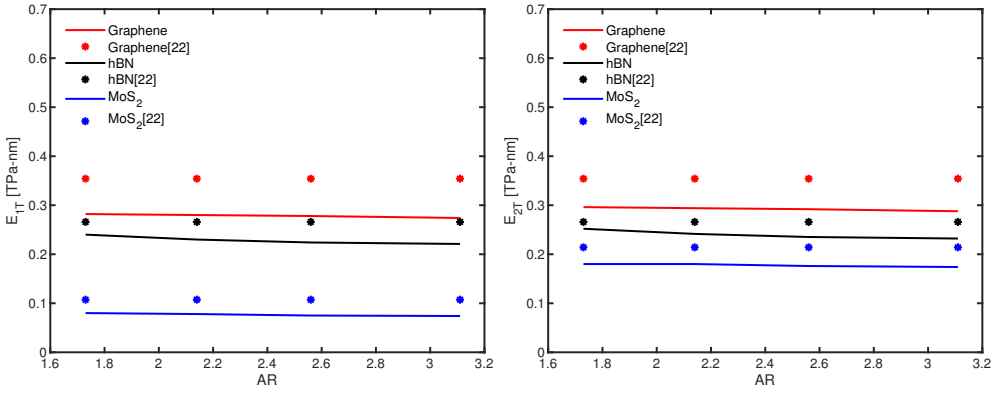

(a) Tensile rigidity in armchair direction (b) Tensile rigidity in zigzag direction

Fig. 6: Variation of tensile rigidity against aspect ratio (AR). Values from atomistic simulations correlated against Ref [20].

4.2. Validation of natural frequencies of graphene-hBN nano hetero-structures

This section involves dynamic analysis of graphene-triple layer hBN nano hetero-structure, wherein three layers of hBN have been overlapped on a single layer of graphene. This configuration has been chosen to validate the present numerical model against the molecular dynamics (MD) model of similar configurations in the literature[19]. Each pair of atoms in adjacent sheets within the bundle have been linked through L-J potential springs. In order to validate the atomistic FE dynamic models, the modal analysis has been performed by constraining two edges of the multi layer nano hetero-structure. Four separate finite element models have been constructed with sheet sizes 5.534 nm $\times$ 12.121 nm, 5.534 nm $\times$ 13.789 nm, 5.534 nm $\times$ 16.121 nm and 5.534nm $\times$ 20.112nm. For these 4 finite element models, the width has remained constant at

Table 4: Results for Young's moduli compared against the values from literature. E_T from the present work is the maximum tensile rigidity among E_{1T} and E_{2T} calculated at four different lengths of sheet (Ref Fig. 6).

Material	Present Results (TPa-nm)	Reference results from literature (E_T in TPa-nm)
Graphene	$E_T = 0.296$	Experimental: 0.34 [35], 0.306 [36] *Ab initio*: 0.350 [37], 0.357 [14], 0.377 [38], 0.364 [39] Molecular Dynamics: 0.357 [40], 0.343 [41] Molecular Mechanics: 0.354 [10], 0.3604 [18] Analytical: 0.354 [20]
hBN	$E_T = 0.252$	Experimental: 0.251 [42] *Ab initio*: 0.271 [37], 0.272 [43] Molecular Dynamics: 0.236 [44], 0.278 [45] Molecular Mechanics: 0.269 [46], 0.322 [47] Analytical: 0.265 [20]
MoS_2	$E_T = 0.18$	Experimental: 0.211 [48], 0.1629 [49] *Ab initio*: 0.141 [50], 0.262 [51] Molecular Dynamics: 0.150 [52] Analytical: 0.21 [20]

5.534 nm and the length has been varied from 12.121 nm to 20.112 nm. These dimensions, boundary conditions and layer combinations have been chosen in order to replicate the MD simulations[19]. The variation of the natural frequencies with respect to the sheet lengths has been shown in Fig. 7. This plot presents two curves: a curve from the current atomistic FE simulations and a curve extracted from the MD results [19]. The trend of variation in the current work is comparable with those of MD simulations[19]. Both atomistic FE and MD simulations predict a drop in natural frequency as the length of multilayer nano hetero-structure sheet is increased. However, the natural frequencies predicted by the atomistic FE simulations are found to be lower than those predicted by MD simulations. This is due to the fact that the number

of numerical approximations happening within the finite element analysis including round off approximations and beam element degrees of freedom (leading to sheet flexibility). At higher lengths, the results of atomistic FE simulations tend to converge towards those of MD simulations. Also, the curve of natural frequencies between the lengths 12.121 nm and 20.112 nm appears to be flattening as compared to the rest of the curve. This further proves that, as the atomistic space frame lattice of nano-strucutures becomes larger in dimension, it simulates a continuous plate as observed by the authors for bilayer and single layer graphene sheets [24].

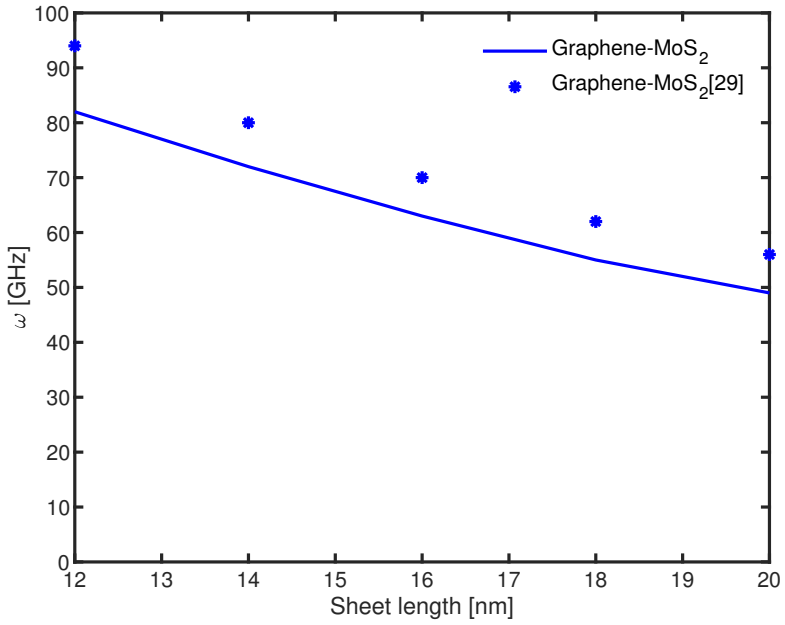

Fig. 7: Comparision of natural frequencies of current work against the values in literature[19].

4.3. Mode shapes of nano hetero-structures

In order to demonstrate the mode shapes associated with fundamental frequencies, the 1st four mode shapes are presented in this section. Prior to enforcing boundary conditions, an initial free-free modal simulation has been carried out to verify the dynamic behaviour of the double layer structures without the influence of external clamps and/or supports. The boundary condition used to perform modal analysis is cantilevered condition (Ref Fig. 10). Cantilever condition involves clamping at one edge and setting free other three edges of the coupled nano sheets. Modal analysis has been performed on graphene-hBN and graphene-MoS_2 nano hetero-structures. Chosen size of both coupled sheets is 10.5 nm $\times$ 3.5 nm. Such a dimension will lead to a nano ribbon type rectangular sheet with an aspect ratio 3. The first four mode shapes for graphene-hBN and graphene-MoS_2 are shown in Fig. 8 and Fig. 9. Here, the first four natural frequencies for graphene-hBN are 122 GHz, 144 GHz, 187 GHz and 202 GHz and for

graphene-MoS_2 the frequencies are 102 GHz, 131 GHz, 154 GHz and 190 GHz. For the case of graphene-hBN, first mode shape is an out of plane bending with a cantilever tip motion, second mode shape is an out of plane bending with single waviness, third mode shape is a torsional twisting mode and the fourth mode shape is an out of plane bending with double waviness. These mode shapes are comparable to that of bilayer graphene [24]. For the case of graphene-MoS_2, first mode shape is an out of plane bending with a cantilever tip motion, second mode shape is a non-homogenous out of plane bending, third mode shape is a non-homogenous twist and fourth mode shape is an out of plane opening mode. Importantly, waviness has been observed in the second mode shapes of graphene–MoS_2. The presence of sheet separation modes (mode II, mode III and mode IV) in graphene-MoS_2, indicates that the layer-layer interaction stiffness (weak van der Waals/L-J potentials) is lower in graphene–MoS_2 as compared to graphene-hBN. It is important to note that the presence of out of plane bond angle (Ref Fig. 1 and Table 1) in MoS_2 reduces the degree of interaction with any adjacent nano sheet. The first mode shapes for graphene-hBN and graphene-MoS_2 are similar. The other three mode shapes for the two types of nano hetero-structures considered here are completely dissimilar.

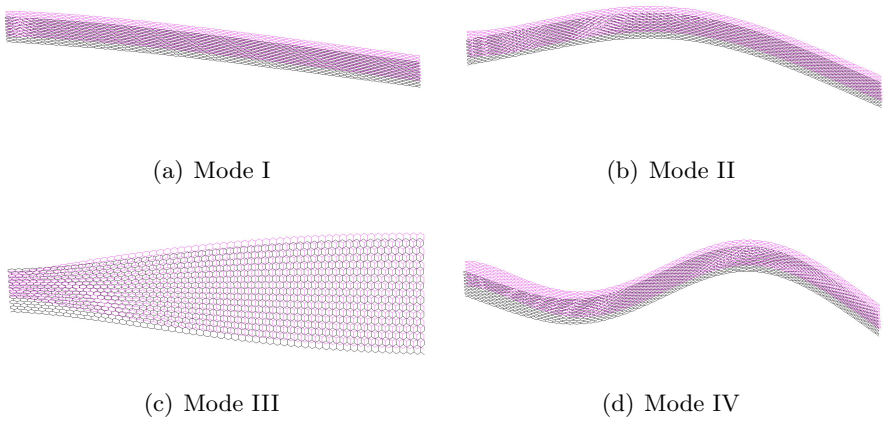

(a) Mode I (b) Mode II

(c) Mode III (d) Mode IV

Fig. 8: First four mode shapes of graphene-hBN nano hetero-structure.

4.4. Dependence on the length and aspect ratio

The resonant frequencies of nano hetero-structures will depend on their geometric configurations. The atomic structures in graphene, hBN and MoS_2 could also exert significant influence on their dynamic behaviours. Thus, in this work, we analyze two groups of hexagonal atomic arrangements, i.e., zigzag and armchair with varying length and width. The results of the fundamental frequencies of armchair and zigzag graphene-hBN are presented in Fig. 11, for bridged

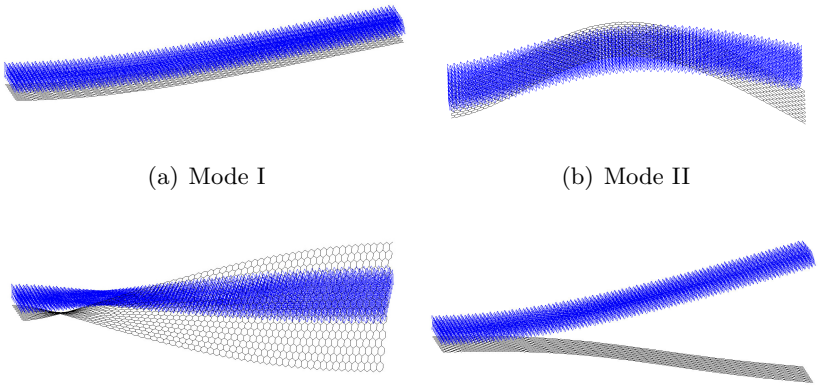

(a) Mode I (b) Mode II

(c) Mode III (d) Mode IV

Fig. 9: First four mode shapes of graphene-MoS_2 nano hetero-structure.

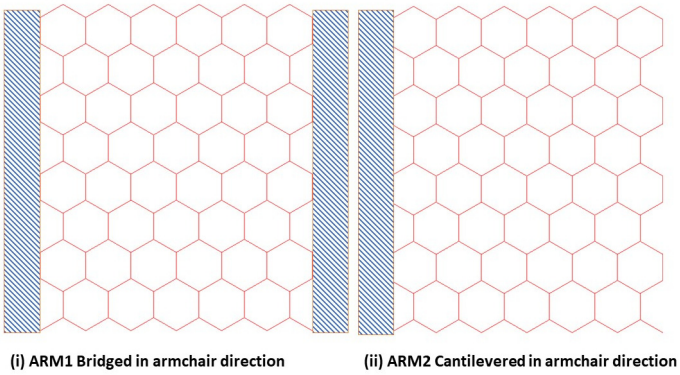

(a) Bridged and Cantilevered in armchair direction

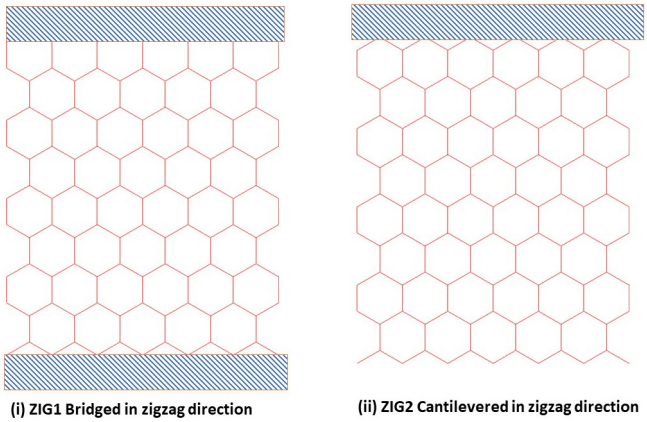

(b) Bridged and Cantilevered in zizag direction

Fig. 10: Depiction of bridged and cantilever boundary conditions (the marked edges are fully constrained in all six degrees of freedom).

and cantilevered boundary conditions. It can be witnessed that for armchair graphene-hBN (width = 4.08 nm) with the increasing length from $\sim 11\mathring{A}$ to $\sim 160\mathring{A}$ have fundamental frequencies in the range between 7-380 GHz for cantilever condition and 82-880 GHz for bridged condition. Zigzag graphene-hBN (width = 4.1 nm) have instead their natural frequencies distributed between 6-233 GHz and 75-680 GHz for cantilevered and bridged boundary conditions respectively, with increasing lengths between $11\mathring{A}$ to $160\mathring{A}$. The trend observed (ref. Fig. 11) is similar to the one identified for single layer graphene [53] and bi layer graphene [24]. The results of the fundamental frequencies of armchair and zigzag graphene-MoS_2 are presented in Fig. 12, for bridged and cantilevered boundary conditions. It can be witnessed that for armchair graphene-MoS_2 (width = 4.08 nm) with the increasing length from $\sim 11\mathring{A}$ to $\sim 160\mathring{A}$ have fundamental frequencies in the range between 5-296 GHz for cantilever condition and 63-680 GHz for bridged condition. Zigzag graphene-hBN (width = 4.1 nm) have instead their natural frequencies distributed between 4-181 GHz and 58-526 GHz for cantilevered and bridged boundary conditions respectively, with increasing lengths between $11\mathring{A}$ to $160\mathring{A}$. The trend observed (ref. Fig. 11) is similar to the one identified for single layer graphene [53] and double layer graphene [24].

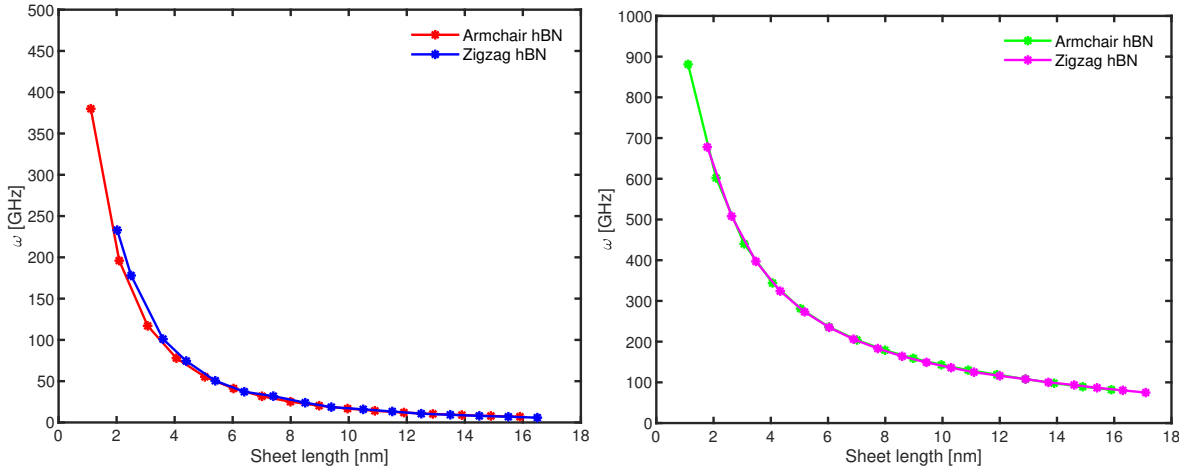

(a) Cantilever model (b) Bridged model

Fig. 11: The dependence of the natural frequency on length: (a) Cantilevered boundary condition - fundamental frequencies of armchair and zigzag graphene-hBN as a function of sheet length. (b) Bridged boundary condition - fundamental frequencies of armchair and zigzag graphene-hBN as a function of sheet length.

In Fig. 13 and Fig. 14, the variations of natural frequencies for graphene-hBN and graphene-MoS_2 with respect to length at a given aspect ratio are displayed. These plots are similar to the ones obtained by Sakhaee-Pour et al [53]. The pattern of variation here is similar to

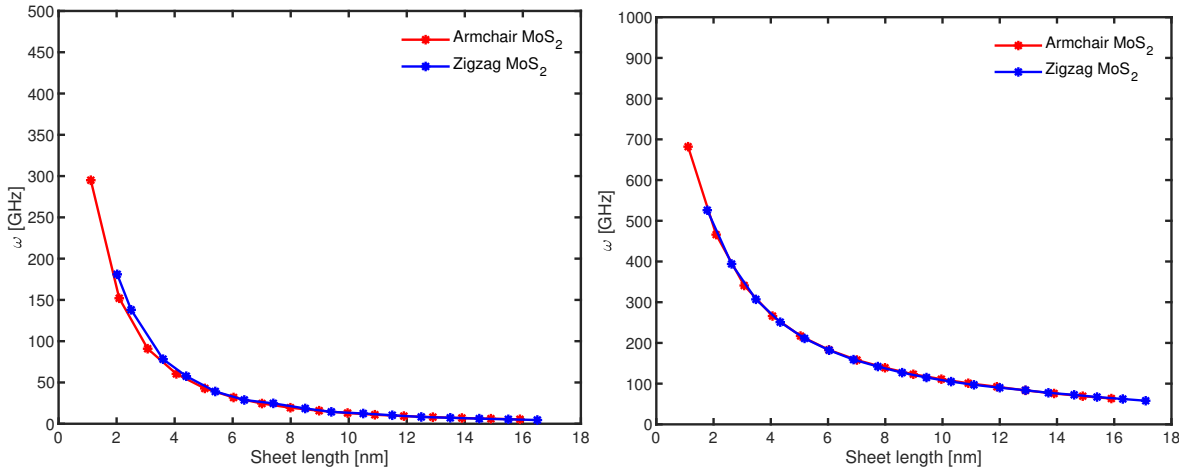

(a) Cantilever model (b) Bridged model

Fig. 12: The dependence of the natural frequency with length: (a) Cantilevered boundary condition - fundamental frequencies of armchair and zigzag graphene-MoS_2 as a function of length. (b) Bridged boundary condition - fundamental frequencies of armchair and zigzag graphene-MoS_2 as a function of length.

that of single [53] and double layer [24] graphene. In Fig. 13, the first value of the frequency associated to an aspect ratio of 0.4 coincides with the second value of natural frequency for aspect ratio 0.52, i.e., at width reduction of about 50 %. Natural frequency is a measure of stiffness of an engineering structure. Graphene being the stiffest among the three nano structures considered here, significantly influences the natural frequency of nano hetero-structures. In general, graphene-hBN nano hetero-structure offers higher natural frequency as compared to graphene-MoS_2 for given length and aspect ratio. This behaviour is in line with stiffness (tensile rigidities) of nano sheets presented in Fig. 6.

4.5. Dependence on the boundary condition

From the point of view of structure mechanics, a bridged structure offers higher natural frequency [54] as compared to the cantilever one. As per Fig. 11 and Fig. 12, the change of the boundary condition from one-edge-fixed to both-edge-fixed enhances the natural frequency upto 3 times. Similar trend has been observed for the second natural frequency for both graphene-hBN and graphene-MoS_2. Clamping the nano hetero-structure sheet at all edges will further enhance the stiffness, and therfore increase the natural frequency. These results suggest that with the increasing of the aspect ratio, the natural frequency of a cantilever model will be lowered at higher rate as compared to a bridged model . From these observations, we can also conclude that the bridged topologies (Ref Fig. 10) are suitable for nano-electro-mechanical-system applications, where resonant frequencies are required to be very high, whereas the cantilever topologies (Ref

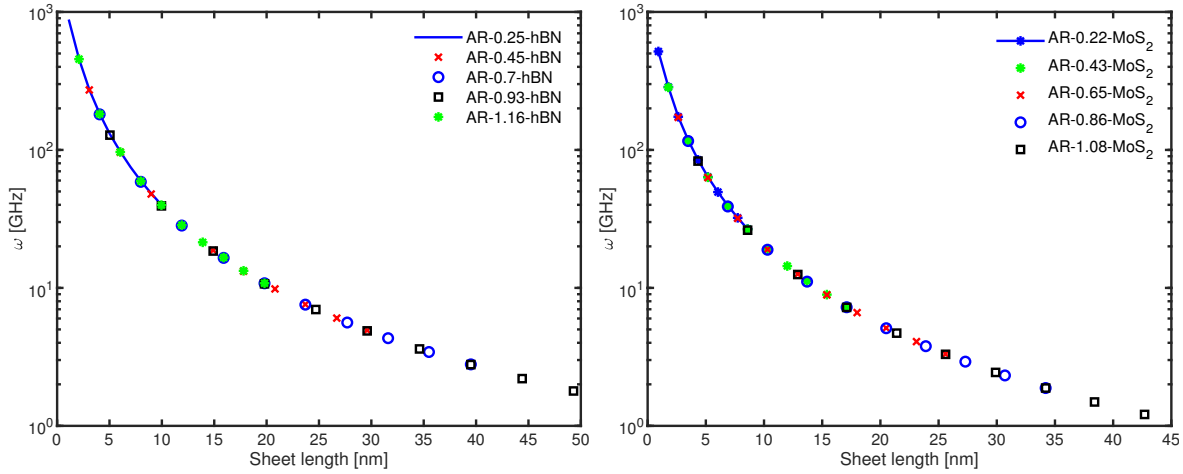

(a) Model-ARM2 (b) Model-ZIG2

Fig. 13: The variation of natural frequencies with length at a given aspect ratio for graphene-hBN nano hetero-structure.

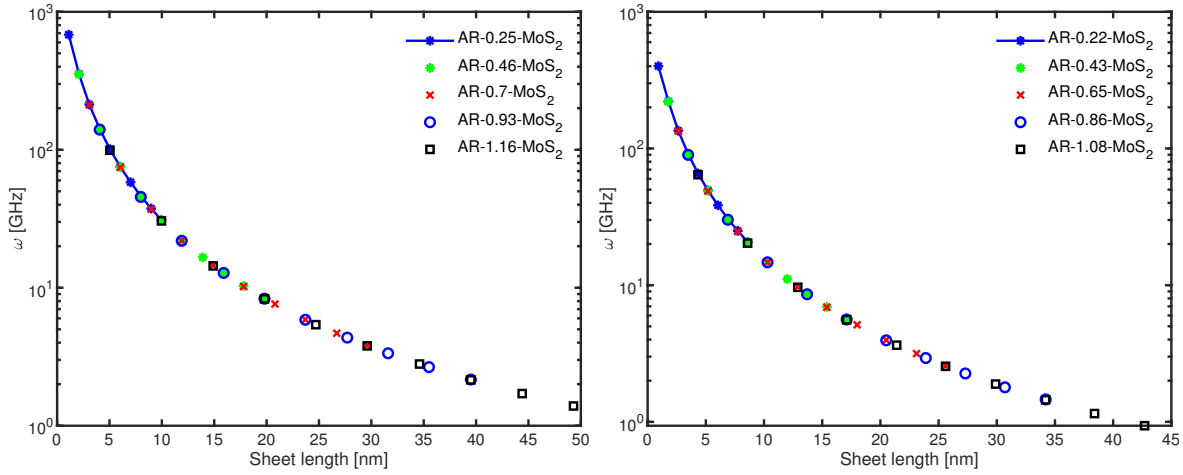

(a) Model-ARM2 (b) Model-ZIG2

Fig. 14: The variation of natural frequencies with length at a given aspect ratio for graphene-MoS_2 nano hetero-structure.

Fig. 10) are suitable for low resonant frequency applications.

4.6. The effect of chirality

As per the results here, chirality is proven to be influencing the natural frequencies of vibration (ref. Fig. 11 and Fig. 12). For a given width and length, the fundamental frequencies of armchair nano hetero-structure sheets are higher than those of zigzag ones. However, increasing the sheet length diminishes the effect provided by the atomic configurations. The maximum relative difference calculated as $(\omega_{zigzag} - \omega_{armchair})/\omega_{armchair}$ is of the order of 0.35 and 0.31 for cantilevered and bridged boundary conditions, respectively. This behavior is not inline with

the difference between the natural frequencies of the two chiral configurations (i.e., zigzag and armchair) of carbon nanotubes (CNTs), since a maximum relative difference being of the order 0.08 [55]. The frequency of CNTs is chiefly influenced by their geometry , i.e., diameter and the aspect ratio, and the atomic structure plays a minor role, specifically for long tubes, resulting in a general good fidelity of classical mechanics models to determine the dynamic behavior of CNTs with different atomic structures. For the case of double layered nano hetero-structures presented here, the natural frequencies are found to be dependent on both the geometric properties and chiralities, at lower dimensions.

5. Conclusions

An atomistic finite element method has been used for the dynamic analysis of graphene-hBN and graphene-MoS_2 nano hetero-structures. Within the atomistic-FE model, the bonds are represented by equivalent structural beams with stretching, bending and torsional capabilities. The proposed numerical models have been validated by performing elastic analysis and also dynamic analysis. The modulii of elasticity predicted by atomistic models of single layers of graphene, hBN and MoS_2 have been validated against analytical, molecular dynamics/mechanics, *ab initio* and experimental solutions available in the literature. The natural frequencies obtained by the atomistic models of graphene-hBN nano hetero-structures have been validated against the solutions of molecular dynamics based simulations available in the literature. The mode shapes of graphene-hBN and graphene-MoS_2 nano hetero-structures have been presented. The weak van der Waals interactions between the layers are found to be influencing the mode shapes. Based on the modulus of elasticities of nano hetero-structures considered here, graphene-hBN offers a higher bending stiffness as compared to graphene-MoS_2, leading to higher natural frequencies. Similar to the behaviour observed in single and bilayer graphene sheets as presented in the literature, the fundamental natural frequency reduces with increasing length and aspect ratio. The bridged models of nano hetero-structures are found to be offering higher natural frequencies as compared to cantilever counterparts, making them more appropriate for high resonance applications. There is no significant difference between the natural frequencies of armchair and zigzag models for large nanosheet configurations, while the chirality considerably influences the dynamics behaviour of nano hetero-structures for lengths lower than 3 nm.

[1] Y. Gan, W. Chu, L. Qiao, Stm investigation on interaction between superstructure and grain boundary in graphite, Surface Science 539 (1) (2003) 120 – 128. doi:https://doi.

org/10.1016/S0039-6028(03)00786-6.
URL http://www.sciencedirect.com/science/article/pii/S0039602803007866

[2] K. S. Novoselov, A. K. Geim, S. V. Morozov, D. Jiang, Y. Zhang, S. V. Dubonos, I. V. Grigorieva, A. A. Firsov, Electric field effect in atomically thin carbon films, Science 306 (5696) (2004) 666–669. arXiv:https://science.sciencemag.org/content/306/5696/666.full.pdf, doi:10.1126/science.1102896.
URL https://science.sciencemag.org/content/306/5696/666

[3] S. Balendhran, S. Walia, H. Nili, S. Sriram, M. Bhaskaran, Elemental analogues of graphene: Silicene, germanene, stanene, and phosphorene, Small 11 (6) (2015) 640–652. arXiv:https://onlinelibrary.wiley.com/doi/pdf/10.1002/smll.201402041, doi:10.1002/smll.201402041.
URL https://onlinelibrary.wiley.com/doi/abs/10.1002/smll.201402041

[4] M. Xu, T. Liang, M. Shi, H. Chen, Graphene-like two-dimensional materials, Chemical Reviews 113 (5) (2013) 3766–3798, pMID: 23286380. arXiv:https://doi.org/10.1021/cr300263a, doi:10.1021/cr300263a.
URL https://doi.org/10.1021/cr300263a

[5] S. Das, J. A. Robinson, M. Dubey, H. Terrones, M. Terrones, Beyond graphene: Progress in novel two-dimensional materials and van der waals solids, Annual Review of Materials Research 45 (1) (2015) 1–27. arXiv:https://doi.org/10.1146/annurev-matsci-070214-021034, doi:10.1146/annurev-matsci-070214-021034.
URL https://doi.org/10.1146/annurev-matsci-070214-021034

[6] A. K. Geim, I. V. Grigorieva, Van der waals heterostructures, Nature 499 (419). doi:https://doi.org/10.1038/nature12385.

[7] Y. J. Zhang, M. Yoshida, R. Suzuki, Y. Iwasa, 2d crystals of transition metal dichalcogenide and their iontronic functionalities, 2D Materials 2 (4) (2015) 044004. doi:10.1088/2053-1583/2/4/044004.
URL https://doi.org/10.1088%2F2053-1583%2F2%2F4%2F044004

[8] A. A. Balandin, S. Ghosh, W. Bao, I. Calizo, D. Teweldebrhan, F. Miao, C. N. Lau, Superior thermal conductivity of single-layer graphene, Nano Letters 8 (3) (2008) 902–907, pMID:

18284217. arXiv:https://doi.org/10.1021/nl0731872, doi:10.1021/nl0731872.
URL https://doi.org/10.1021/nl0731872

[9] F. Scarpa, S. Adhikari, A. S. Phani, Effective elastic mechanical properties of single layer graphene sheets, Nanotechnology 20 (6) (2009) 065709. doi:10.1088/0957-4484/20/6/065709.
URL https://doi.org/10.1088%2F0957-4484%2F20%2F6%2F065709

[10] M. M. Shokrieh, R. Rafiee, Prediction of youngs modulus of graphene sheets and carbon nanotubes using nanoscale continuum mechanics approach, Materials & Design 31 (2) (2010) 790 – 795. doi:https://doi.org/10.1016/j.matdes.2009.07.058.
URL http://www.sciencedirect.com/science/article/pii/S026130690900421X

[11] L. Boldrin, F. Scarpa, R. Chowdhury, S. Adhikari, Effective mechanical properties of hexagonal boron nitride nanosheets, Nanotechnology 22 (50) (2011) 505702. doi:10.1088/0957-4484/22/50/505702.
URL https://doi.org/10.1088%2F0957-4484%2F22%2F50%2F505702

[12] V. Zolyomi, J. R. Wallbank, V. I. Falko, Silicane and germanane: tight-binding and first-principles studies, 2D Materials 1 (1) (2014) 011005. doi:10.1088/2053-1583/1/1/011005.
URL https://doi.org/10.1088%2F2053-1583%2F1%2F1%2F011005

[13] T. Lorenz, J.-O. Joswig, G. Seifert, Stretching and breaking of monolayer MoS2—an atomistic simulation, 2D Materials 1 (1) (2014) 011007. doi:10.1088/2053-1583/1/1/011007.
URL https://doi.org/10.1088%2F2053-1583%2F1%2F1%2F011007

[14] F. Liu, P. Ming, J. Li, Ab initio calculation of ideal strength and phonon instability of graphene under tension, Phys. Rev. B 76 (2007) 064120. doi:10.1103/PhysRevB.76.064120.
URL https://link.aps.org/doi/10.1103/PhysRevB.76.064120

[15] R. Grantab, V. B. Shenoy, R. S. Ruoff, Anomalous strength characteristics of tilt grain boundaries in graphene, Science 330 (6006) (2010) 946–948. arXiv:https://science.sciencemag.org/content/330/6006/946.full.pdf, doi:10.1126/science.1196893.
URL https://science.sciencemag.org/content/330/6006/946

[16] E. W. Bucholz, S. B. Sinnott, Mechanical behavior of mos2 nanotubes under compression, tension, and torsion from molecular dynamics simulations, Journal of Applied Physics 112 (12) (2012) 123510. arXiv:https://doi.org/10.1063/1.4769739, doi:10.1063/1.4769739.
URL https://doi.org/10.1063/1.4769739

[17] E. W. Bucholz, S. B. Sinnott, Structural effects on mechanical response of mos2 nanostructures during compression, Journal of Applied Physics 114 (3) (2013) 034308. arXiv:https://doi.org/10.1063/1.4815879, doi:10.1063/1.4815879.
URL https://doi.org/10.1063/1.4815879

[18] T. Chang, H. Gao, Size-dependent elastic properties of a single-walled carbon nanotube via a molecular mechanics model, Journal of the Mechanics and Physics of Solids 51 (6) (2003) 1059 – 1074. doi:https://doi.org/10.1016/S0022-5096(03)00006-1.
URL http://www.sciencedirect.com/science/article/pii/S0022509603000061

[19] J. Zhang, Vibrations of van der waals heterostructures: A study by molecular dynamics and continuum mechanics, Journal of Applied Physics 125 (2) (2019) 025113. arXiv:https://doi.org/10.1063/1.5064421, doi:10.1063/1.5064421.
URL https://doi.org/10.1063/1.5064421

[20] T. Mukhopadhyay, A. Mahata, S. Adhikari, M. A. Zaeem, Effective elastic properties of two dimensional multiplanar hexagonal nanostructures, 2D Materials 4 (2) (2017) 025006. doi:10.1088/2053-1583/aa551c.
URL https://doi.org/10.1088%2F2053-1583%2Faa551c

[21] B. Gelin, Molecular modeling of polymer structures and properties., Hanser Gardner Publications,.

[22] C. Li, T.-W. Chou, A structural mechanics approach for the analysis of carbon nanotubes, International Journal of Solids and Structures 40 (10) (2003) 2487 – 2499. doi:https://doi.org/10.1016/S0020-7683(03)00056-8.
URL http://www.sciencedirect.com/science/article/pii/S0020768303000568

[23] Y. Chandra, R. Chowdhury, S. Adhikari, F. Scarpa, Elastic instability of bilayer graphene using atomistic finite element, Physica E: Low-dimensional Systems and Nanostructures

44 (1) (2011) 12 – 16. doi:https://doi.org/10.1016/j.physe.2011.06.020.
URL http://www.sciencedirect.com/science/article/pii/S1386947711002232

[24] Y. Chandra, R. Chowdhury, F. Scarpa, S. Adhikaricor, Vibrational characteristics of bilayer graphene sheets, Thin Solid Films 519 (18) (2011) 6026 – 6032. doi:https://doi.org/10.1016/j.tsf.2011.04.012.
URL http://www.sciencedirect.com/science/article/pii/S0040609011008248

[25] Y. Chandra, R. Chowdhury, F. Scarpac, S. Adhikarib, J. Sienza, C. Arnoldd, T. Murmu, D. Boulda, Vibration frequency of graphene based composites: A multiscale approach, Materials Science and Engineering B 177 (2012) 303 310. doi:http://dx.doi.org/10.1016/j.mseb.2011.12.024.

[26] Y. Chandra, F. Scarpa, R. Chowdhury, S. Adhikari, J. Sienz, Multiscale hybrid atomistic-fe approach for the nonlinear tensile behaviour of graphene nanocomposites, Composites Part A 46 (2013) 147–153. doi:https://doi.org/10.1016/j.compositesa.2012.11.006.

[27] Y. Chandra, F. Scarpa, S. Adhikari, J. Zhang, E. Flores, H. Peng, Pullout strength of graphene and carbon nanotube/epoxy composites, Composites Part B 102 (1-8). doi:http://dx.doi.org/10.1016/j.compositesb.2016.06.070.

[28] Y. Chandra, E. Saavedra-Flores, F. Scarpa, S. Adhikari, Buckling of hybrid nano composites with embedded graphene and carbon nanotubes, Physica E 83 (2016) 434–441. doi:http://dx.doi.org/10.1016/j.physe.2016.01.021.

[29] F. Scarpa, S. Adhikari, R. Chowdhury, The transverse elasticity of bilayer graphene, Physics Letters A 374 (19) (2010) 2053 – 2057. doi:https://doi.org/10.1016/j.physleta.2010.02.063.
URL http://www.sciencedirect.com/science/article/pii/S0375960110002240

[30] L. A. Girifalco, M. Hodak, R. S. Lee, Carbon nanotubes, buckyballs, ropes, and a universal graphitic potential, Phys. Rev. B 62 (2000) 13104–13110. doi:10.1103/PhysRevB.62.13104.
URL https://link.aps.org/doi/10.1103/PhysRevB.62.13104

[31] J.-W. Jiang, H. S. Park, Mechanical properties of mos2/graphene heterostructures, Applied Physics Letters 105 (3) (2014) 033108. arXiv:https://doi.org/10.1063/1.4891342,

doi:10.1063/1.4891342.
URL https://doi.org/10.1063/1.4891342

[32] R. M. Elder, M. R. Neupane, T. L. Chantawansri, Stacking order dependent mechanical properties of graphene/mos2 bilayer and trilayer heterostructures, Applied Physics Letters 107 (7) (2015) 073101. arXiv:https://doi.org/10.1063/1.4928752, doi:10.1063/1.4928752.
URL https://doi.org/10.1063/1.4928752

[33] A. J. Pak, G. S. Hwang, Theoretical analysis of thermal transport in graphene supported on hexagonal boron nitride: The importance of strong adhesion due to π-bond polarization, Phys. Rev. Applied 6 (2016) 034015. doi:10.1103/PhysRevApplied.6.034015.
URL https://link.aps.org/doi/10.1103/PhysRevApplied.6.034015

[34] M. Neek-Amal, F. M. Peeters, Graphene on boron-nitride: Moir pattern in the van der waals energy, Applied Physics Letters 104 (4) (2014) 041909. arXiv:https://doi.org/10.1063/1.4863661, doi:10.1063/1.4863661.
URL https://doi.org/10.1063/1.4863661

[35] C. Lee, X. Wei, J. W. Kysar, J. Hone, Measurement of the elastic properties and intrinsic strength of monolayer graphene, Science 321 (5887) (2008) 385–388. arXiv:https://science.sciencemag.org/content/321/5887/385.full.pdf, doi:10.1126/science.1157996.
URL https://science.sciencemag.org/content/321/5887/385

[36] B. Demczyk, Y. Wang, J. Cumings, M. Hetman, W. Han, A. Zettl, R. Ritchie, Direct mechanical measurement of the tensile strength and elastic modulus of multiwalled carbon nanotubes, Materials Science and Engineering: A 334 (1) (2002) 173 – 178. doi:https://doi.org/10.1016/S0921-5093(01)01807-X.
URL http://www.sciencedirect.com/science/article/pii/S092150930101807X

[37] K. N. Kudin, G. E. Scuseria, B. I. Yakobson, c_2F, bn, and c nanoshell elasticity from ab initio computations, Phys. Rev. B 64 (2001) 235406. doi:10.1103/PhysRevB.64.235406.
URL https://link.aps.org/doi/10.1103/PhysRevB.64.235406

[38] G. V. Lier, C. V. Alsenoy, V. V. Doren, P. Geerlings, Ab initio study of the elastic properties of single-walled carbon nanotubes and graphene, Chemical Physics Letters 326 (1) (2000)

181 – 185. doi:https://doi.org/10.1016/S0009-2614(00)00764-8.
URL http://www.sciencedirect.com/science/article/pii/S0009261400007648

[39] D. Sánchez-Portal, E. Artacho, J. M. Soler, A. Rubio, P. Ordejón, Ab initio structural, elastic, and vibrational properties of carbon nanotubes, Phys. Rev. B 59 (1999) 12678–12688. doi:10.1103/PhysRevB.59.12678.
URL https://link.aps.org/doi/10.1103/PhysRevB.59.12678

[40] J.-W. Jiang, J.-S. Wang, B. Li, Young's modulus of graphene: A molecular dynamics study, Phys. Rev. B 80 (2009) 113405. doi:10.1103/PhysRevB.80.113405.
URL https://link.aps.org/doi/10.1103/PhysRevB.80.113405

[41] H. Zhao, K. Min, N. R. Aluru, Size and chirality dependent elastic properties of graphene nanoribbons under uniaxial tension, Nano Letters 9 (8) (2009) 3012–3015, pMID: 19719113. arXiv:https://doi.org/10.1021/nl901448z, doi:10.1021/nl901448z.
URL https://doi.org/10.1021/nl901448z

[42] L. Song, L. Ci, H. Lu, P. B. Sorokin, C. Jin, J. Ni, A. G. Kvashnin, D. G. Kvashnin, J. Lou, B. I. Yakobson, P. M. Ajayan, Large scale growth and characterization of atomic hexagonal boron nitride layers, Nano Letters 10 (8) (2010) 3209–3215, pMID: 20698639. arXiv:https://doi.org/10.1021/nl1022139, doi:10.1021/nl1022139.
URL https://doi.org/10.1021/nl1022139

[43] Q. Peng, W. Ji, S. De, Mechanical properties of the hexagonal boron nitride monolayer: Ab initio study, Computational Materials Science 56 (2012) 11 – 17. doi:https://doi.org/10.1016/j.commatsci.2011.12.029.
URL http://www.sciencedirect.com/science/article/pii/S0927025611006902

[44] S. Zhao, J. Xue, Mechanical properties of hybrid graphene and hexagonal boron nitride sheets as revealed by molecular dynamic simulations, Journal of Physics D: Applied Physics 46 (13) (2013) 135303. doi:10.1088/0022-3727/46/13/135303.
URL https://doi.org/10.1088%2F0022-3727%2F46%2F13%2F135303

[45] M.-Q. Le, Young's modulus prediction of hexagonal nanosheets and nanotubes based on dimensional analysis and atomistic simulations, Meccanica 49 (7) (2014) 1709–1719. doi:10.1007/s11012-014-9976-z.
URL https://doi.org/10.1007/s11012-014-9976-z

[46] L. Jiang, W. Guo, A molecular mechanics study on size-dependent elastic properties of single-walled boron nitride nanotubes, Journal of the Mechanics and Physics of Solids 59 (6) (2011) 1204 – 1213. doi:https://doi.org/10.1016/j.jmps.2011.03.008.
URL http://www.sciencedirect.com/science/article/pii/S0022509611000536

[47] E.-S. Oh, Elastic properties of various boron-nitride structures, Metals and Materials International 17 (1) (2011) 21–27. doi:10.1007/s12540-011-0204-2.
URL https://doi.org/10.1007/s12540-011-0204-2

[48] A. Castellanos-Gomez, M. Poot, G. A. Steele, H. S. J. van der Zant, N. Agrat, G. Rubio-Bollinger, Elastic properties of freely suspended mos2 nanosheets, Advanced Materials 24 (6) (2012) 772–775. arXiv:https://onlinelibrary.wiley.com/doi/pdf/10.1002/adma.201103965, doi:10.1002/adma.201103965.
URL https://onlinelibrary.wiley.com/doi/abs/10.1002/adma.201103965

[49] S. Bertolazzi, J. Brivio, A. Kis, Stretching and breaking of ultrathin mos2, ACS Nano 5 (12) (2011) 9703–9709, pMID: 22087740. arXiv:https://doi.org/10.1021/nn203879f, doi:10.1021/nn203879f.
URL https://doi.org/10.1021/nn203879f

[50] T. Lorenz, D. Teich, J.-O. Joswig, G. Seifert, Theoretical study of the mechanical behavior of individual tis2 and mos2 nanotubes, The Journal of Physical Chemistry C 116 (21) (2012) 11714–11721. arXiv:https://doi.org/10.1021/jp300709w, doi:10.1021/jp300709w.
URL https://doi.org/10.1021/jp300709w

[51] E. Scalise, M. Houssa, G. Pourtois, V. Afanas'ev, A. Stesmans, Strain-induced semiconductor to metal transition in the two-dimensional honeycomb structure of mos2, Nano Research 5 (1) (2012) 43–48. doi:10.1007/s12274-011-0183-0.
URL https://doi.org/10.1007/s12274-011-0183-0

[52] J.-W. Jiang, Z. Qi, H. S. Park, T. Rabczuk, Elastic bending modulus of single-layer molybdenum disulfide (MoS2): finite thickness effect, Nanotechnology 24 (43) (2013) 435705. doi:10.1088/0957-4484/24/43/435705.
URL https://doi.org/10.1088%2F0957-4484%2F24%2F43%2F435705

[53] A. Sakhaee-Pour, M. T. Ahmadian, R. Naghdabadi, Vibrational analysis of single-layered graphene sheets, Nanotechnology 19 (8) (2008) 085702. doi:10.1088/0957-4484/19/8/

085702.
URL https://doi.org/10.1088%2F0957-4484%2F19%2F8%2F085702

[54] G. B. Warburton, The vibration of rectangular plates, Proceedings of the Institution of Mechanical Engineers 168 (1) (1954) 371–384. arXiv:https://doi.org/10.1243/PIME_PROC_1954_168_040_02, doi:10.1243/PIME_PROC_1954_168_040_02.
URL https://doi.org/10.1243/PIME_PROC_1954_168_040_02

[55] R. Chowdhury, S. Adhikari, C. Wang, F. Scarpa, A molecular mechanics approach for the vibration of single-walled carbon nanotubes, Computational Materials Science 48 (4) (2010) 730 – 735. doi:https://doi.org/10.1016/j.commatsci.2010.03.020.
URL http://www.sciencedirect.com/science/article/pii/S0927025610001382